

Oil-Fat Mixtures with Low Solid Fat Concentration: Influence of Fat Concentration and Cooling Conditions

Stefan B. Irmscher¹ · Monika Gibis¹ · Kurt Herrmann¹ · Reinhard Kohlus² · Jochen Weiss¹

Received: 24 June 2013 / Revised: 27 May 2015 / Accepted: 28 June 2015 / Published online: 9 August 2015
© AOCS 2015

Abstract Uniform suspension of particulates (salt or spices) in oil-based marinades requires a gel behavior of the matrix. This can be achieved by adding a solid fat to the liquid oil. Besides rheology, appearance and thermal stability are important for the utilization as marinades. The influence of solid fat concentration ($c_{\text{fat}} = 2.5\text{--}5.5$ wt%) and average cooling speed (1.4, 2.6, and 4.7 °C/min) on the functional properties of oil-fat gels from palm fat and canola oil was investigated. Oil-fat mixtures showed complex physiochemical behavior depending on the solid fat concentration and cooling rate. All samples had a shear-thinning behavior. Yield stresses and apparent viscosities increased at a constant cooling rate with increasing solid fat concentration. Frequency dependence of storage and loss modulus showed a transition from a viscous solution to a weak gel at $c_{\text{fat}} > 3.5$ wt%. Samples at increasing cooling rates transitioned to weak gels at lower fat concentration (2.5 wt%). Mixtures became turbid and increasingly whiter as both solid fat concentration and cooling rates increased, which was explained by increased light-scattering by fat crystal aggregates. Results show the critical importance of proper formulation and preparation conditions on the functionality of oil-based marinades.

Keywords Fat crystal networks · Solid fat concentration · Cooling conditions · Rheological properties · Microstructure · Thermal stability · Appearance

Introduction

The purpose of meat marination is to provide flavor, color and to enhance the yield and quality of meat products [1]. Aside from the sometimes used injection of marinades into meats, marinades are most commonly used to cover the surface of meats prior to grilling or roasting. Marinades may generally consist of simple dry spice rubs or liquid blends with water, oil or a mixture of water and oil [1, 2]. Oil-fat gels are extremely useful systems in the production of marinades. In contrast to spice rubs and oil-in-water marinades, they entrap meat juices better during grilling and, therefore, reduce yield losses [3, 4]. They are ideal carriers for lipophilic aromatics and antioxidants which may prevent the formation of heterocyclic aromatic amines, as well as pigments, such as paprika oleoresin. Moreover, they may be formulated in such a way that they are transparent, which allows the underlying meat muscle structure to be seen through the marinade. They provide a gloss to the surface of meats upon application that is attractive to many consumers. The engineering of appropriate rheological properties is of particular importance for marinades, since marinades must have, on the one hand, sufficiently high viscosities so as to keep the spices and salt suspended, but, on the other hand be able to be pumped for automated dosing and packaging of products [1, 2].

The viscosity of water-based marinades can be adjusted by the addition of hydrocolloids, in particular, starch as well as cold-swelling gums such as xanthan or guar gum [1, 2]. Several strategies of structuring edible oils have

Submitted to the Journal of the American Oil Chemists' Society in January, 2015

✉ Jochen Weiss
j.weiss@uni-hohenheim.de

¹ Department of Food Physics and Meat Science, Institute of Food Science and Biotechnology, University of Hohenheim, Garbenstrasse 21/25, 70599 Stuttgart, Germany

² Department of Process Engineering and Food Powders, Institute of Food Science and Biotechnology, University of Hohenheim, Garbenstrasse 25, 70599 Stuttgart, Germany

been investigated over the past years. Organogelators such as fatty acids, fatty alcohols, wax esters, mixtures of lecithin and sorbitan tristearate, as well as mixtures of phytosterol and oryzanol have been found to be useful to prepare edible oil gels [5–9]. Moreover, the oil phase in many food products, including margarine, shortenings, butter, lard, spreads, ice cream, peanut butter, and chocolate, is structured by solid lipids that form a complex three-dimensional fat crystal network [10].

Fat crystal networks may be formed from hot melts of mixtures of solid fat and liquid oil. Upon cooling, stable nuclei are formed that may grow with continuous cooling, and Kloek *et al.* [11] for example determined nucleation kinetics for fully hydrogenated palm oil/sunflower oil mixtures. Once formed, fat crystals may aggregate to form bigger fat crystal flocs due to Van der Waals attraction between the individual colloidal crystal particles. The attractive interaction of flocculated lipid crystals may, subsequently, lead to the formation of a three-dimensional network, which is able to entrap lipid phases that have not precipitated from the melt upon cooling [12–17]. Over time and if crystals are physically close enough, sintering between the crystals may occur, permanently fixating the network and providing it with a higher stiffness and rigidity [18]. Recently, the description of the structural hierarchy of fat crystal networks was expanded by the distinction of a mesoscale and nanoscale structure. The mesoscale structure constitutes the microstructural level of fat crystal networks at a length scale of 1–200 μm whereas the nanoscale is dominated by single crystal platelets having size ranges of several hundred nanometers [19–21].

Several attempts have been made over the past years to describe the properties of fat crystal-based mixtures using model systems [22–25]. The microstructure of fat crystal networks, in particular, the underlying crystalline form may be altered by the solid fat content and the crystallization conditions. Thus, rheological properties may be adjusted by alteration of solid fat concentration and/or cooling rate [26–30]. These studies have particularly focused on oil-fat mixtures that had high solid fat contents with <10 wt% solid fat, due to the fact that the authors were interested in describing the physicochemical behavior of high solid fat products, such as chocolate and butter. By contrast, much less information about the physicochemical properties of oil-fat mixtures with low solid fat contents is available.

Only a few studies have dealt with low solid fat content oil-fat mixtures, particularly the group of Higaki *et al.* [31–33] prepared oil-fat gels from a hot mixture of high-melting fats with low-melting fats. Upon crystallization, they prepared oil-fat gels with a variety of high-melting fats, such as fully hydrogenated canola oil behenic acid or stearic acid, tristearoyl-glycerol, triarachidonoyl-glycerol, and tribehenoyl-glycerol. Sal fat olein, cocoa butter,

palm super olein, and olive oil were used as low-melting lipids. The authors reported the formation of oil-fat gels at high-melting fat concentrations below 2.0 wt% after tempering of the samples, i.e., after samples were repeatedly heated and cooled causing a polymorphic transition from α - to β -crystals. A simple cooling, however, did not suffice to form functional oil-fat mixtures with gel-like behavior [31]. They investigated the crystal morphology of the oil-fat gels with 2 wt% high-melting fat during the temperature process and concluded that crystal morphology was influenced by the TAG composition of the high-melting fat, the viscosity of the low-melting component and the tempering process [32]. In a subsequent study, the authors determined the rheological properties of a high-melting fat at solid fat concentrations up to 4 wt% and reported the formation of oil gels during cool quenching [33]. They hypothesized that cool quenching led to the formation of smaller, more numerous β -crystals that, in turn, formed a more extended network.

The industrial production of marinades demands an easy-to-produce process like a simple cooling to manufacture oil-fat gels with desirable functional properties. The objective of this study was to investigate the influence of solid fat concentration and cooling conditions more systematically, including not only the mechanical, but also the optical and thermal behavior of the oil-fat mixtures. We hypothesize that the thermal and mechanical stability could be optimized without changes of the transparent optical properties of the oil-fat mixtures. Oil-fat mixtures were prepared from hot melts of palm fat with canola oil by controlled cooling at various cooling rates. The mechanical behavior of oil-fat mixtures was assessed by steady and oscillatory shear rheometry. The appearance of systems was determined by colorimetry, while thermal properties were measured by differential scanning calorimetry. Finally, crystal size and network structure were investigated by cross-polarized light microscopy.

Materials and Methods

Materials

Hydrogenated palm fat (Sett[®] P55) was donated by Cognis (Monheim, Germany) and used as the solid fat in the studies. The palm fat had an iodine value of max. 4.0 and a melting range of 55–60 $^{\circ}\text{C}$, according to the specifications of the manufacturer. The density of the hydrogenated palm fat was $\rho_{\text{palm fat}} = 0.926 \text{ g/cm}^3$. Canola oil was obtained from Bunge (Mannheim, Germany), had a density of $\rho_{\text{canola oil}} = 0.926 \text{ g/cm}^3$, and was used as the liquid oil phase. Both lipids were used as received without further purification.

Preparation of Oil-Fat Mixtures

Oil-fat mixtures were prepared by melting palm fat at 2.5–5.5 wt% in canola oil at 80 °C. The temperature was held for 30 min at 80 °C to erase crystal memory. Crystallization was induced by cooling the hot molten oil-fat mixture at three different cooling rates (1.4, 2.6, and 4.7 °C/min) to a temperature of 10 °C using a refrigerated water bath filled with a saturated sodium chloride solution (F25, Julabo, Allentown, PA, USA). The water bath was set to 10, 0, and –10 °C to allow for three different cooling rates to be achieved. Average cooling speeds were calculated from the time required to reach the target temperature and varied by less than ± 0.2 °C/min upon repetitions of the studies. Samples were mildly stirred while cooling at less than approximately 100 rpm using a stirrer to improve heat transfer and ensure a uniform temperature distribution in the sample. The surface and core temperature were measured with a thermometer (Type Almemo 2290-8, Ahlborn, Holzkirchen, Germany) equipped with two NiCr-Ni thermowires (Type ZA 9020-FS, Ahlborn, Holzkirchen, Germany). The surface temperature varied from the core temperature by less than 0.3 °C. When samples had reached a temperature of 10 °C they were transferred to another water bath having been set at 10 °C. There they were allowed to equilibrate for 1 h. Finally, samples were stored at 25 °C for 48 h until analyses were performed.

Rheological Measurements

A modular compact oscillatory rheometer MCR300 (Anton Paar, Stuttgart, Germany) with the application software Rheoplus/32 V3.31 (Anton Paar) was equipped with a parallel plate–plate measurement system (PP-50, plate diameter: 50 mm), and a gap setting of 0.5 mm was used to perform all rheological experiments. Samples were carefully transferred to the rheometer and were allowed to equilibrate for 5 min after lowering the upper plate. Flow behavior was measured by increasing the shear rate of the plate–plate system at 25 °C logarithmically from 0.02 to 100 s⁻¹. The mechanical stability of the samples during heating was assessed by recording the shear stresses when the samples were heated from 20–60 °C at a heating rate of 7.2 °C/min and sheared at a shear rate of 1 s⁻¹. In addition, a coaxial cylinder system was used to accurately measure the viscosities of samples that had been completely melted (CC-27, cup diameter: 28.92 mm, bob diameter: 26.66 mm). The viscoelastic behavior of the samples was assessed by an oscillating frequency sweep from 0.05 to 10 Hz at 2 % strain and 25 °C. Prior to the frequency sweeps, amplitude sweeps had been conducted to ensure that oscillation studies were conducted within the linear viscoelastic regime (LVE). Since the LVE extended to 5 % strain for even the

strongest oil gel manufactured, oscillation measurements within the 2 % strain rate fell within the LVE (data not shown).

Differential Scanning Calorimetry (DSC)

The thermal behavior of oil-fat mixtures was recorded using a Perkin Elmer DSC 8500 (Perkin Elmer, CT, USA). An amount of 10–20 mg of the sample was placed in a 20- μ l aluminum pan; the pans were sealed, the sample weight recorded, the pans inserted in the DSC, and heated from 20 to 60 °C at a rate of 20 °C/min. Prior to the temperature scan, samples were equilibrated for 5 min at 20 °C. Enthalpy of melting was calculated by integration of the heat-flow rate during the phase transition, taking the weight of the added palm fat into account.

Optical Analysis

L^* , a^* , and b^* values in the CIE tristimulus color space were measured at 25 °C using a chromameter CR-200 (Konica Minolta, Marunouchi, Japan) to determine the optical properties of the samples. The chromameter was calibrated against a white calibration plate with tristimulus values: $Y = 93.7$, $x = 0.3159$, $y = 0.3321$ at D_{65} illumination. The samples were measured with the measurement port of the chromameter immersed in the sample at five different positions, maintaining a sample layer thickness of 2 cm against a white background. Results for lightness (L^*) were normalized against the lightness of pure palm fat ($L_0^* = 96.61$) by calculating the ratio of L^*/L_0^* .

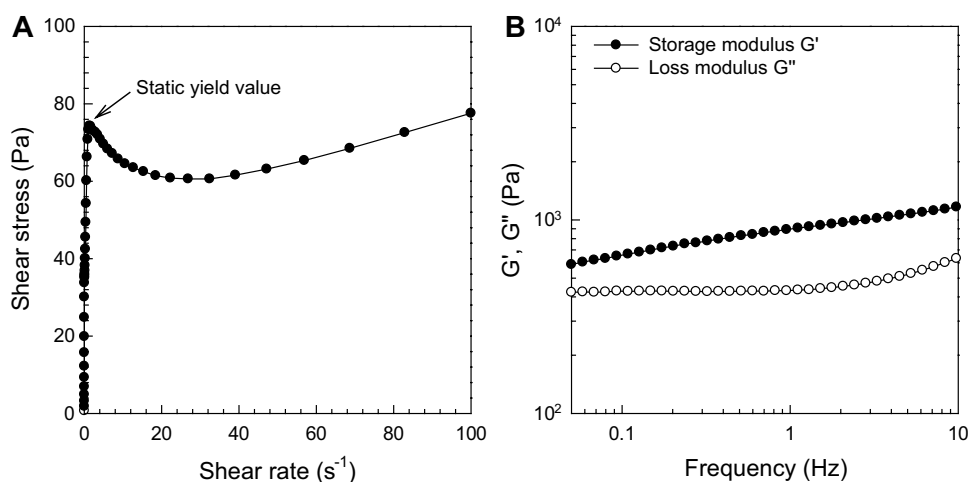
Determination of Microstructure

Polarized light microscopy images for the determination of crystal structure and size were taken with an axial-mounted Canon Powershot G10 digital camera (Canon, Tokyo, Japan) mounted on an Axio Scope A1 optical microscope (Carl Zeiss Microimaging GmbH, Göttingen, Germany). Samples of approximately 0.5 mg were carefully placed on an objective slide using a spatula, and covered with a thin glass cover. Care was taken to avoid excessive compression by the glass cover. Images were taken at a magnification of 200. Images were processed and analyzed with Gimp 2.6.6 (GIMP Development Team, USA) and Imagej 1.43 n (Wayne Rasband, National Institutes of Health, USA).

Low Resolution Nuclear Magnetic Resonance Spectroscopy

Solid fat content was determined at 25 °C with a Bruker minispec mq20 TD-NMR Analyzer (Bruker Corp., Billerica, MA, USA) equipped with a pulsed gradient field

Fig. 1 Shear stress vs shear rate (a) and elastic moduli vs frequency at a 2 % strain (b) of an oil-fat mixture containing 4.5 wt% palm fat in canola oil subjected to a cooling rate of 2.6 °C/min



unit. The hydrogenated palm fat/canola oil mixtures were placed in an NMR tube and equilibrated at 25 °C for 30 s. The amount of solid fat was determined by measuring the difference in signal decay between solid and liquid fraction after applying a 90° electromagnetic pulse. At least six measurements were conducted per sample.

Statistical Analysis

Measurements were replicated at least three times using duplicate samples. Mean values and standard deviations were calculated using Excel (Microsoft, Redmond, CA). Nonlinear regression fits for the calculation of regression parameters and coefficients of determination were carried out using OriginPro 8 (Northampton, MA, USA).

Results and Discussion

Physicochemical Properties of a Base Oil-Fat Mixture

Initially, we determined the optical, microstructural, rheological, and thermal properties of a base oil-fat mixture composed of hydrogenated palm fat as the dispersed phase and canola oil. This initial base oil-fat mixture was prepared by cooling a hot melt containing 4.5 wt% palm fat at a cooling rate of 2.6 °C/min. A base oil-fat mixture with a solid fat content of 4.5 % was chosen to investigate the physicochemical properties of a system with a gel-like behavior. The palm fat concentration was also chosen based on the concentration of a commercially available oil-fat gel based marinade. There, the manufacturer had observed that the system was able to keep salt and spices used for the formulation of marinades in suspension, and that the mixture could still be pumped to cover the steaks prior to packaging. In the following sections we investigated how the physicochemical properties

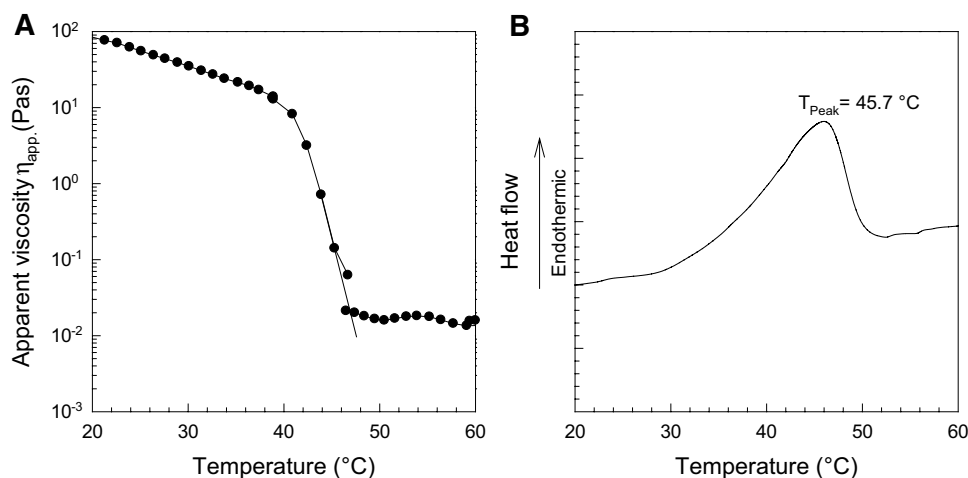
were impacted by solid fat concentration and cooling conditions.

Results of the steady shear experiments are plotted in Fig. 1A. The oil-fat mixture displayed a strong shear-thinning behavior, i.e., the viscosity during the continuous shear experiment decreased continuously as the shear rate increased. The flow curve had a characteristic peak at a critical shear rate, which is typical for plastic fats. This kind of behavior has been reported previously for lards, margarines, and shortenings [34].

The formation of crystal flocs may be attributed to strong primary bonds or weaker secondary bonds. The primary bonds are due to crystals having fused together or having been connected by sintered fat bridges during crystallization. Whereas the secondary bonds are due to attractive Van der Waals interactions between individual fat crystal flocs [15]. Upon applying a strain to the oil-fat mixture, the bonds between crystal flocs stretch elastically. Beyond a certain maximal shear stress, the primary bonds may break. Secondary bonds may be disrupted simultaneously. The maximal shear stress at which primary bonds are broken is referred to as the “static yield value” [34–36]. The breakage of the primary bonds is generally irreversible whereas the weaker secondary bonds may reform when the sample comes to rest [15, 37, 38]. When the critical deformation that corresponds to the static yield stress is exceeded, the fat crystal network is irreversibly disrupted. The subsequent decrease in shear stress upon further deformation is indicative of the structure breakdown and is referred to as “work-softening” [37–39]. In our oil-fat mixture, the static yield value was 74.3 Pa at a shear rate of 1.35 s⁻¹. In the work-softening region, where the sample behaved more like a suspension, the apparent viscosity of the sample at shear rate of 39 s⁻¹ was 1.58 Pa·s.

Oscillatory rheological measurements of G' and G'' (Fig. 1B) indicated that the system behaved like a gel. The term gel typically describes an infinite network where the

Fig. 2 Apparent viscosity η_{app} with shearing at 1 s^{-1} (a) and heat flow determined by differential scanning calorimetry (b) as a function of temperature (20–60 °C) of an oil-fat mixture containing 4.5 wt% palm fat in canola oil subjected to a cooling rate of 2.6 °C/min



structure percolates through the entire macroscopic sample. In food systems though, the term gel may sometimes be used more loosely describing a viscoelastic system that exhibits a more elastic than viscous behavior with $G' > G''$ over a certain frequency range. The sample had large elastic and storage moduli that ranged from 300 to more than 1000 Pa at frequencies ranging from 0.05 to 10 Hz with G' being larger than G'' , confirming that the sample had more solid than fluid properties. Calculations of the phase angle indicated that the oil-fat gel had phase angles that were all well below 45° over the entire frequency range [40, 41]. Higaki *et al.* observed similar results for samples prepared with fully hydrogenated high behenic canola oil using a tempering process [33].

The thermal behavior of the oil-fat gel was determined by heating the sample in the rheometer from 20 to 60 °C at a shear rate of 1 s^{-1} and by DSC analysis during the heating of the sample from 20 to 60 °C, shown in Fig. 2. Viscosity of the oil-fat gel generally decreased when the oil-fat gel was heated. At 40.9 °C, the viscosity of the oil-fat gel dropped sharply by almost three magnitudes over a temperature range of approximately 6 °C. The structure that had been created during crystallization of solid fat and formation of a fat crystal network was completely lost at temperatures above 47 °C because the solid fat crystals had completely melted. It should be noted that the viscosity of the melt was too low to be measured by the plate–plate system. Hence, the viscosity of the completely liquefied oil-fat gel was measured with a separate coaxial cylinder measurement system. The viscosity of the melt was found to decrease from 0.02 to 0.01 Pa·s due to a temperature-dependent viscosity loss. The liquefaction temperature, i.e., the temperature at which the structure given by the fat crystal network was lost, was determined from the cross-point of the asymptote of the melting curve determined with the plate–plate geometry and the viscosity of the oil-fat melt determined with the coaxial cylinder measurement system,

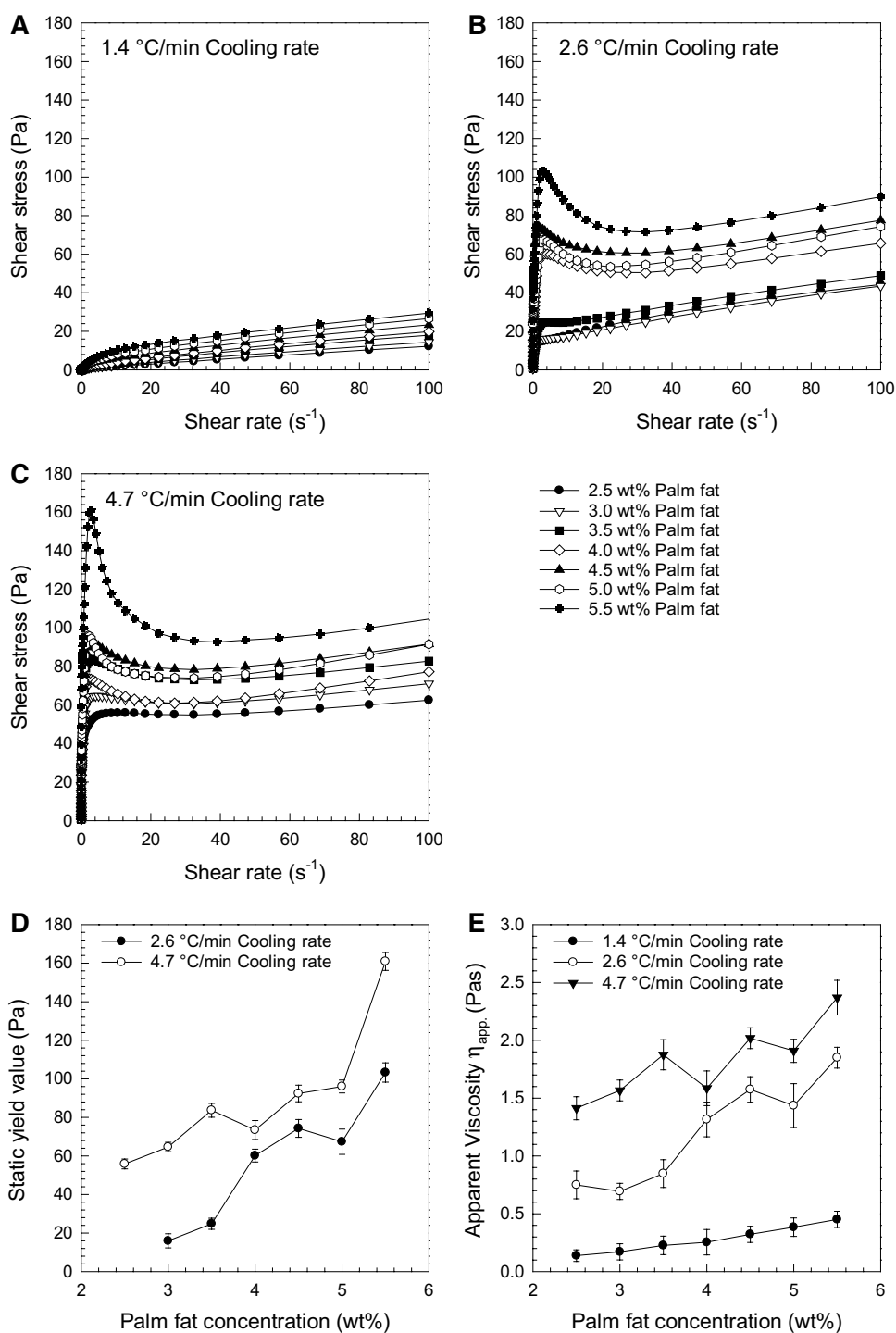
and was found to be 46.9 °C. A DSC analysis indicated that the melting of fat crystals started at an onset temperature of 35.7 °C with the peak of the melting of fat crystals occurring at 45.7 °C, which is in good agreement with the rheological results. The enthalpy of melting of the sample measured was 159.40 J/g.

The generated oil-fat gel was nearly transparent, that is it had extremely low lightness values, i.e., $L^* = 36.92 \pm 1.03$ [$a^* = -0.64 \pm 0.24$ and $b^* = 1.41 \pm 1.32$]. Cross-polarized light microscopic images of the oil-fat mixture allowed the microstructure of the fat crystal network to be visualized. The microstructure represents the mesoscale in the fat crystal network and is constituted of aggregates that are formed by crystal clusters [42]. An automated analysis by image analysis was not possible. Consequently, an analysis of the images was conducted by individually determining the dimensions of the fat crystal aggregates and by counting the crystal aggregates on each image. The crystal aggregate diameter of fats in the oil-fat mixture prepared with 4.5 wt% palm fat varied between 5 and 10 μm . Light-scattering theory for spherical particles predicts a local minimum in the intensity of scattered light at this approximate size range, which may explain the transparency of the oil-fat gel observed, a fact that is also apparent from the low L^* value. Oil droplets in oil-in-water emulsions are known to maximally scatter light at oil droplet diameters of approximately 1 μm with scattering intensities decreasing above and below this critical diameter [43].

Influence of Solid Fat Concentration

Next, we investigated the influence of solid fat concentration on the physicochemical properties of oil-fat mixtures which had been subjected to a cooling rate of 2.6 °C/min . The concentration of palm fat was varied from 2.5 to 5.5 wt% by increments of 0.5 % to prepare oil-fat mixtures

Fig. 3 Shear stress vs shear rate of oil-fat mixtures subjected to different cooling rates at 1.4 °C/min (a), 2.6 °C/min (b), and 4.7 °C/min (c) with varying palm fat concentration (2.5–5.5 wt%) in canola oil; static yield value (d), and apparent viscosity η_{app} at a shear rate of 39.1 s^{-1} (e) vs palm fat concentration in canola oil



with a lower and higher solid fat concentrations than in the base oil-fat gel.

The flow behavior of the oil-fat mixtures containing varying palm fat concentrations is shown in Fig. 3A-C. Flow curves of the samples with 2.5 to 5.5 wt% palm fat subjected to an intermediate cooling rate of 2.6 °C are shown in Fig. 3B. The shear stress and apparent viscosity increased with increasing palm fat concentration. Apparent viscosity

at a shear rate of 39.1 s^{-1} was $0.75 \text{ Pa}\cdot\text{s}$ for $c_{fat} = 2.5 \text{ wt}\%$ and increased to $1.85 \text{ Pa}\cdot\text{s}$ for $c_{fat} = 5.5 \text{ wt}\%$. The steady yield stress (Fig. 3D) increased with the increasing concentration of palm fat, while no peak was observed at 2.5 wt%. This increase of the static yield stress with the increasing palm fat concentration suggested a larger number of primary bonds which may be attributed to a larger number of lipid bridges between fat crystals and sintered crystals due

Table 1 Storage G' and loss G'' moduli and phase angle $\delta = \arctan(G''/G') \cdot 180^\circ \times \pi$ at an oscillation frequency of 1.1 Hz of oil-fat mixtures subjected to different cooling rates at 1.4, 2.6, and 4.7 °C/min as a function of palm fat concentration in canola oil (2.5–5.5 wt%)

Cooling rate (°C/min)	Palm fat concentration c_{fat} (wt%)	G' (Pa)	G'' (Pa)	δ (°)
1.4	2.5	0.4	1.3	72.9
	3.0	0.5	1.9	75.3
	3.5	1.7	2.7	57.8
	4.0	2.1	3.5	59.0
	4.5	2.4	3.9	58.4
	5.0	2.0	4.8	67.4
	5.5	1.9	3.7	62.8
2.6	2.5	97.8	53.5	28.5
	3.0	59.6	62.7	46.5
	3.5	162.3	121.7	36.9
	4.0	512.2	306.3	30.9
	4.5	907.4	434.2	25.6
	5.0	1706.0	700.0	22.3
	5.5	626.7	316.7	26.8
4.7	2.5	588.2	171.9	16.3
	3.0	701.1	292.6	22.7
	3.5	909.1	339.2	20.5
	4.0	778.6	356.6	24.6
	4.5	1230.0	459.2	20.5
	5.0	1160.0	638.8	28.8
	5.5	1265.0	715.3	29.5

to the higher number of crystals present in the oil-fat gels. Thus, the more palm fat available for the structuring of the oil-fat gels, the more extensive and the stronger the three-dimensional network.

The viscoelasticity of oil-fat mixtures generally increased with increasing palm fat concentration, i.e., storage G' and loss G'' modulus increased while phase angle δ decreased. Table 1 shows G' , G'' , and the phase angle δ ($= \arctan(G''/G') \cdot 180^\circ/\pi$) at an oscillation frequency of 1.1 Hz for oil-fat mixtures that had different fat concentrations and were cooled at 2.6 °C/min. When the palm fat concentration exceeded a critical concentration of 3.5 wt% at this cooling rate, the properties of the oil-fat mixtures transitioned from a viscous behavior typical for a suspension to a weak gel characteristic for a particle network. That is, G' became larger than G'' or, in other words, the phase angle decreased below 45° [40, 41]. A transition from a viscous to a mainly elastic system with increasing solid fat concentration has also been reported for blends of refined bleached deodorized palm oil with 4–25 wt% hydrogenated palm oil [44]. The study was focused on determining changes in mechanical properties of a selected oil-fat mix over time; however, initial experiments were

also conducted to assess the impact of mixing ratio. The authors stated that an increase in complex viscosities, compression force, and hardness index suggested that the crystal networks of the blends became more structured with a higher concentration of hydrogenated palm oil; for example, upon the addition of 18 wt% hydrogenated palm oil, the complex viscosity increased by a factor of 6 and the phase angle decreased by a factor of 4.

The thermal stability of oil-fat mixtures during heating from 20 to 60 °C in the rheometer at a shear rate of 1 s^{-1} increased with the increasing concentration of palm fat (Fig. 4A). At a palm fat concentration of 2.5 wt%, the liquefaction temperature, as defined by the intersection between the asymptote of the melting curve and the viscosity of the molten oil-fat mixtures, was 44.5 °C and increased to 48.9 °C at $c_{\text{fat}} = 5.5 \text{ wt}\%$ (Fig. 4B). This small but significant change in the liquefaction temperature and, thus, the small increase in temperature stability was confirmed by the results of the DSC analysis shown in Fig. 4C. The DSC melting curve of the oil-fat mixture with 2.5 wt% palm fat had a peak temperature of 43.06 °C, while the peak temperature for the 5.5 wt% palm fat oil-fat gel was 48.04 °C. This increase in temperature stability was also seen in the onset temperatures in Table 2. No significant difference in the enthalpy of melting of oil-fat mixtures manufactured with varying palm fat concentrations was found. This was to be expected as the enthalpy of melting was measured related to the amount of palm fat added to the sample. A similar increase in temperature stability with increasing solid fat concentrations was also observed in blends of palm oil and hydrogenated palm oil where the slip melting point was found to increase [44]. In a system consisting of a high-melting fat in a low-melting fat, the clear point mainly depends on the solubility of the solid fat in the liquid oil phase which increases with higher temperatures. Hence, clear point temperature of the prepared oil-fat mixtures increased with increasing palm fat concentration [45].

The influence of the palm fat concentration on the optical properties, especially on the transparency of the samples, was again determined by $L^* a^* b^*$ color measurement. With an increasing concentration of palm fat, the lightness and, with it, the normalized L^*/L_0^* increased from 0.34 at $c_{\text{fat}} = 2.5 \text{ wt}\%$ to 0.41 at $c_{\text{fat}} = 5.5 \text{ wt}\%$ (Fig. 5). The optical properties of a system containing dispersed solid or liquid particles depends on the size of the particles, concentration, and refractive index between the two phases [46]. In this series of experiments, only the concentration of palm fat was varied, while the refractive index and the size of crystals (see microscopy images below) remained constant. The results correspond with results of Chantrapornchai *et al.* which showed that light-scattering and, therefore, the lightness and the turbidity

Fig. 4 Apparent viscosity η_{app} with shearing at 1 s^{-1} as function of temperature (20–60 °C) (a), liquefaction temperature determined from viscosity measurements as a function of palm fat concentration in canola oil (b), and heat flow vs temperature determined by differential scanning calorimetry (c) of oil-fat mixtures containing 2.5–5.5 wt% palm fat in canola oil subjected to a cooling rate of 2.6 °C/min

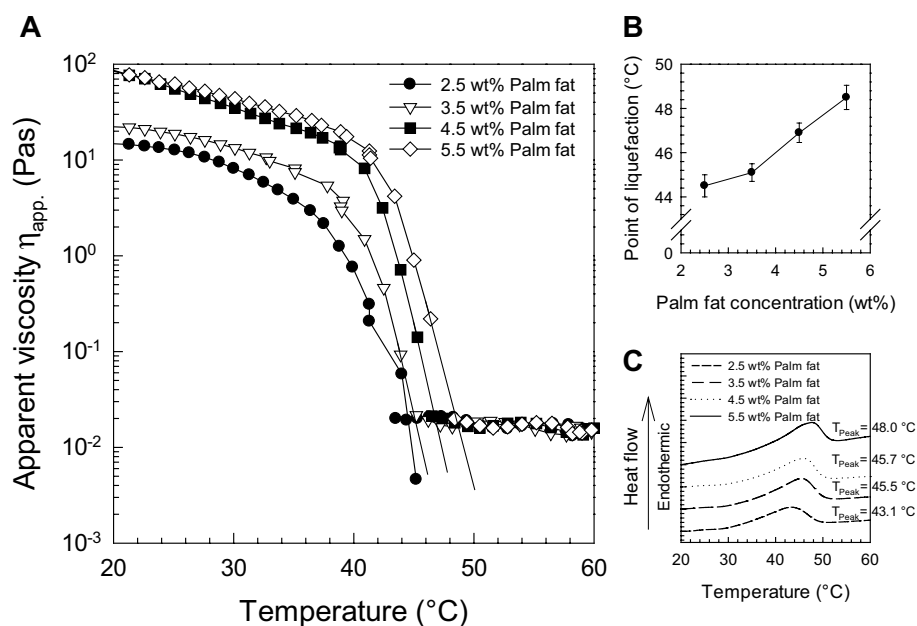


Table 2 Onset (T_{Onset}), peak (T_{Peak}) temperature, and enthalpy of melting (ΔH) at melt transition for oil-fat mixtures with varying palm fat concentration (2.5–5.5 wt%) in canola oil subjected to different cooling rates at 1.4, 2.6, and 4.7 °C/min

Cooling rate (°C/min)	Palm fat concentration c_{fat} (wt%)	Onset temperature T_{Onset} (°C)	Peak temperature T_{Peak} (°C)	Enthalpy of melting ΔH (J/g)
1.4	2.5	41.22 ± 5.01	49.11 ± 0.12	136.31 ± 5.06
	3.5	37.75 ± 1.06	49.48 ± 0.04	150.78 ± 1.15
	4.5	36.28 ± 1.83	49.33 ± 0.37	147.95 ± 4.47
	5.5	37.28 ± 1.82	50.27 ± 0.12	153.40 ± 7.45
2.6	2.5	31.56 ± 0.20	43.06 ± 0.06	146.95 ± 2.51
	3.5	34.40 ± 0.45	45.46 ± 0.12	151.72 ± 1.09
	4.5	35.66 ± 0.23	45.69 ± 0.17	159.40 ± 4.85
	5.5	38.15 ± 1.38	48.04 ± 0.86	146.29 ± 5.52
4.7	2.5	32.59 ± 0.34	43.04 ± 0.09	149.90 ± 6.24
	3.5	34.11 ± 0.10	45.55 ± 0.42	160.41 ± 3.41
	4.5	35.98 ± 0.60	45.97 ± 0.51	160.06 ± 1.71
	5.5	36.39 ± 0.83	46.72 ± 0.73	171.06 ± 8.99

are increased with the increasing concentration of droplets. Although the results of Chantrapornchai *et al.* were for oil-in-water emulsions, the underlying physics is similar [47]. The oil droplets as scattering particles in the emulsions have a similar influence on the transparency and lightness to the fat crystals which scatter the light in our oil-fat mixtures.

Polarized light microscopy images in Fig. 6 showed that increases in the number of crystal aggregates occurred as the concentration of the palm fat in the oil-fat mixtures increased. The crystal aggregate sizes were, however, not affected by increases in the concentration of solid fat, that is, they ranged again from 5 to 10 μm .

Influence of Cooling Rate

The influence of the cooling rate was assessed by cooling the hot melt of canola oil and hydrogenated palm fat at three different cooling rates (1.4, 2.6, and 4.7 °C/min). The impact of the cooling rate on the optical properties, microstructure, rheology, and temperature stability was determined for oil-fat mixtures containing palm fat concentrations that varied between 2.5 and 5.5 wt%.

Cooling conditions led to large alterations in the rheological behavior of the oil-fat mixtures (Fig. 3A–C). All samples underwent shear thinning when deformed regardless of preparation conditions and solid fat concentration. Viscosity

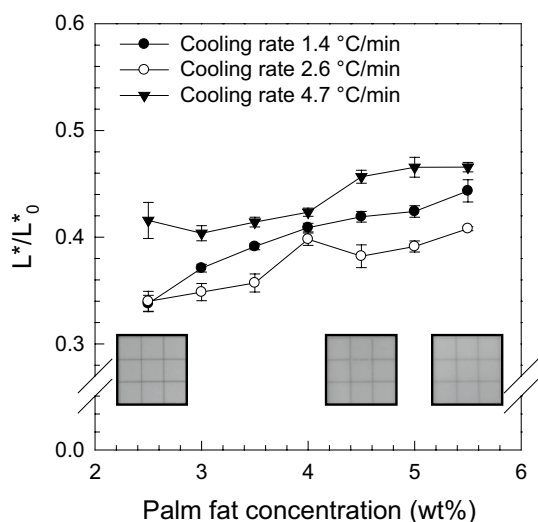
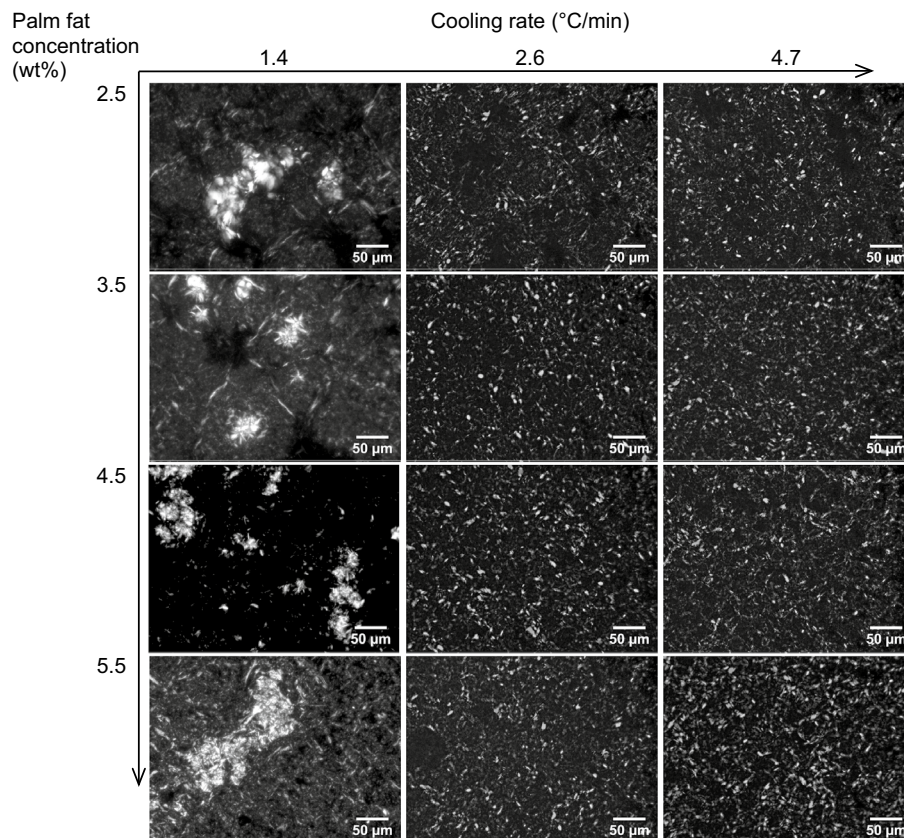


Fig. 5 Normalized lightness L^*/L_0^* of oil-fat mixtures containing varying palm fat concentration (2.5–5.5 wt%) in canola oil subjected to different cooling rates at 1.4, 2.6, and 4.7 °C/min; the inserted images provide photographic images of oil-fat mixtures with 2.5, 4.5, and 5.5 wt% palm fat subjected to a cooling rate of 2.6 °C/min (oil-fat mixture layer thickness: 1.5 mm)

Fig. 6 Polarized light microscopy images at a magnification of 200 \times of oil-fat mixtures subjected to different cooling rates at 1.4, 2.6, and 4.7 °C/min with varying palm fat concentration (2.5–5.5 wt%) in canola oil (scale bar: 50 μ m)



generally increased with higher solid fat concentration regardless of cooling rates used. However, samples that had been produced at slower cooling rates had substantially lower viscosities; for example, at a palm fat concentration of 4.5 wt%, the apparent viscosity was 0.32 Pa·s at 1.4 °C/min, 1.58 Pa·s at 2.6 °C/min and 2.02 Pa·s at 4.7 °C/min (Fig. 3E). More importantly, oil-fat mixtures that had been manufactured at the slowest cooling rate had no static yield stress (Fig. 3D), even at the highest fat concentration used. This suggests that the rheological behavior in the samples cooled at the slowest rate containing large unconnected crystal aggregates never transitioned from a suspension rheology to a plastic fat rheology. By contrast, the samples subjected to the higher cooling rates featured a static yield stress. In addition to the increase of the static yield stress with the solid fat concentration, the static yield stress increased also with higher cooling rates. This may be promoted by a higher number of nuclei upon a more rapid cooling. There, the higher number of fat crystals may induce more numerous primary bonds. The presence of a stress maxima during shearing exists also in entangled polymer solutions and melts where a stress overshoot may be observed during startup shear [48, 49].

Table 3 Fitted Herschel-Bulkley parameters yield stress τ_0 , consistency k , and flow index n of oil-fat mixtures with varying palm fat concentration (2.5–5.5 wt%) in canola oil subjected to different cooling rates (1.4, 2.6, and 4.7 °C/min)

Cooling rate (°C/min)	Palm fat concentration c_{fat} (wt%)	Yield stress τ_0 (Pa)	Consistency k (Pa·s)	Flow index n (–)	R^2
1.4	2.5	0.122 ± 0.027	0.235 ± 0.012	0.854 ± 0.012	0.998
	3.0	0.073 ± 0.031	0.390 ± 0.018	0.779 ± 0.010	0.998
	3.5	0.085 ± 0.047	0.657 ± 0.031	0.714 ± 0.011	0.998
	4.0	0.177 ± 0.044	0.786 ± 0.030	0.695 ± 0.009	0.998
	4.5	0.176 ± 0.093	1.605 ± 0.083	0.571 ± 0.012	0.996
	5.0	–0.035 ± 0.084	2.256 ± 0.080	0.529 ± 0.008	0.998
	5.5	–0.412 ± 0.148	3.183 ± 0.150	0.482 ± 0.011	0.996
2.6	2.5	0.884 ± 0.779	8.964 ± 0.889	0.325 ± 0.020	0.979
	3.0	–0.370 ± 1.114	10.017 ± 1.273	0.294 ± 0.025	0.966
	3.5	–4.921 ± 2.719	20.549 ± 3.007	0.186 ± 0.023	0.957
	4.0	–0.6·10 ⁵ ± 2.0·10 ⁷	0.6·10 ⁵ ± 2.0·10 ⁷	8.2·10 ^{–5} ±0.028	0.874
	4.5	–2.1·10 ⁵ ± 7.9·10 ⁷	2.1·10 ⁵ ± 7.9·10 ⁷	2.7·10 ^{–5} ±0.010	0.844
	5.0	–0.5·10 ⁵ ± 1.5·10 ⁷	0.5·10 ⁵ ± 1.5·10 ⁷	9.8·10 ^{–5} ±0.027	0.886
	5.5	–2.4·10 ⁵ ± 0.000	2.4·10 ⁵ ± 0.000	2.9·10 ^{–5} ±0.000	0.800
4.7	2.5	–0.5·10 ⁵ ± 0.8·10 ⁷	0.5·10 ⁵ ± 0.8·10 ⁷	9.6·10 ^{–5} ±0.014	0.966
	3.0	–0.6·10 ⁵ ± 1.5·10 ⁷	0.6·10 ⁵ ± 1.5·10 ⁷	9.7·10 ^{–5} ±0.026	0.919
	3.5	–1.7·10 ⁵ ± 4.7·10 ⁷	1.7·10 ⁵ ± 4.7·10 ⁷	4.0·10 ^{–5} ±0.011	0.881
	4.0	–1.0·10 ⁵ ± 5.3·10 ⁷	1.0·10 ⁵ ± 5.3·10 ⁷	6.4·10 ^{–5} ±0.036	0.861
	4.5	–0.2·10 ⁵ ± 0.2·10 ⁷	0.2·10 ⁵ ± 0.2·10 ⁷	3.6·10 ^{–4} ±0.029	0.874
	5.0	–2.6·10 ⁵ ± 0.000	2.6·10 ⁵ ± 0.000	2.7·10 ^{–5} ±0.000	0.825
	5.5	–5.0·10 ⁵ ± 0.000	5.0·10 ⁵ ± 0.000	1.8·10 ^{–5} ±0.000	0.706

In order to further analyze the differences between samples, flow curves were fitted with the Herschel-Bulkley model [50] according to Eq. (1):

$$\tau = \tau_0 + k \cdot (\dot{\gamma})^n \quad (1)$$

where τ is the shear stress (Pa), τ_0 is the yield stress (Pa), k is the consistency index (Pa·s), $\dot{\gamma}$ is the shear rate (s^{–1}), and n is the flow index. The Herschel-Bulkley model is the most widely used model to fit flow curves [40]. However, it should be noted that the Herschel-Bulkley model does not account for the presence of static yield stresses, and is typically best suited to fit the behavior of dispersions such as emulsions and suspensions at low particle concentrations that display simple shear thinning behavior. Increases in coefficients of determination R^2 can, therefore, be used to assess deviations from a simple shear thinning behavior. The results for the fitted Herschel-Bulkley model are shown in Table 3. The Herschel-Bulkley model fitted the data at the slowest cooling rate (1.4 °C/min) with minimal errors ($R^2 > 0.99$), regardless of solid fat concentration. In the more slowly cooled oil-fat mixtures, the consistency index k increased with increasing palm fat concentration, while the flow index n decreased with increasing solid fat concentration. This behavior is again characteristic for emulsions and suspensions that contain increasingly higher concentrations of particles [50].

The Herschel-Bulkley model increasingly deviated from the measured flow curves with increasing cooling rates and R^2 values were substantially lower than for the more slowly cooled samples. R^2 values decreased with increasing fat concentrations from 0.97 to as little as 0.71 for oil gels that had been fabricated at cooling rates of 2.6 and 4.7 °C/min. This correlated with the fact that oil-fat gels manufactured with the two higher cooling rates had static yield values (Fig. 3D) which increased with increasing palm fat concentration. This indicated that the samples subjected to higher cooling rates exhibited a more plastic fat rheology rather than a suspension-like flow behavior resulting in an increasing deviation from the Herschel-Bulkley model.

Oscillatory rheological measurements yielded similar results (Table 1). At slow cooling rates (1.4 °C/min), the oil-fat mixtures had the lowest values of G' and G'' . Furthermore, the phase angles of the oil-fat mixtures ranged from 75 to 57°, indicating that all samples behaved more like a viscous fluid than an elastic solid [40, 41]. By contrast, samples subjected to higher cooling rates of 2.6 and 4.7 °C/min exhibited a more elastic than viscous behavior. The samples had significantly higher storage (G') and loss (G'') moduli than at the lowest cooling rate. The rheological character of oil-fat mixtures prepared at a cooling rate of 2.6 °C/min transitioned from a viscous to an elastic solids behavior at a palm fat concentration of 3.5 wt%. In

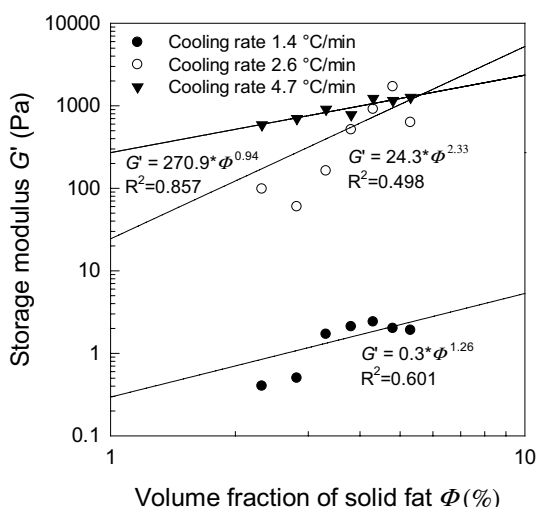


Fig. 7 Storage modulus G' at a frequency of 1.1 Hz as a function of volume fraction of solid fat Φ ; fitted with the power law relation $G' = \gamma \cdot \Phi^m$ equations and R^2 for oil-fat mixtures subjected to the three different cooling rates (1.4, 2.6, and 4.7 °C/min) are in the graph

contrast, the oil-fat mixtures subjected to a cooling rate of 4.7 °C/min all behaved like elastic solids displaying phase angles well below 45° [40, 41]. Thus, the critical concentration for particle network formation decreased to 2.5 wt% palm fat when mixtures were subjected to a cooling rate of 4.7 °C/min. Vreeker *et al.* found that the elastic modulus of fat crystal networks conducted in a similar way to the elasticity of colloidal gels [14]. Thus, they interpreted their rheological data using a power law relationship developed for colloidal gels at low particle concentrations [51]. This model describes a power law relationship between the elastic modulus G' and the particle volume fraction Φ . According to Bremer *et al.*, the equation can be written as [52]:

$$G' = \gamma \Phi^m \quad (2)$$

with m as the power law exponent and γ as a constant independent of volume fraction but dependent on the size of primary particles and the interactions between these particles. This equation has already been used to characterize various types of fat crystal networks [10]. A log G' –log Φ graph was plotted for the cooling rates of 1.4, 2.6, and 4.7 °C/min, Fig. 7. We fitted these oscillatory rheological data using the model mentioned above which resulted in three equations. The amount of solid fat in the oil-fat mixtures was not affected by the cooling rate to which the samples were subjected to. The solid fat content exhibited no significant differences at equal concentrations, e.g., at oil-fat mixtures with 4.5 wt% palm fat the determined solid fat content was 3.6 ± 0.2 % in oil-fat mixtures subjected to a cooling rate of 1.4 °C/min, 3.8 ± 0.2 % in oil-fat gels subjected to a cooling rate of 2.6 °C/min, and 3.9 ± 0.2 % in oil-fat gels subjected to 4.7 °C/min. The particle volume

fraction Φ was calculated from palm fat concentration in the oil-fat mixtures taking the densities of the hydrogenated palm fat and the canola oil into account. Additionally, the theoretical soluble solid fraction 0.17 wt% according to the Hildebrand equation [45, 53] at 25 °C was subtracted from the palm fat concentrations.

$$\ln x_{HP} = \frac{\Delta H_{f,i}}{R_g} \left(\frac{1}{T_{m,i}} - \frac{1}{T} \right) \quad (3)$$

with x_{HP} the mole fraction of hydrogenated palm fat that is soluble at temperature T , $\Delta H_{f,i}$ the molar enthalpy of fusion of polymorph i , R_g is the gas constant ($8.314 \text{ J mol}^{-1} \text{ K}^{-1}$), $T_{m,i}$ is the absolute melting temperature of pure polymorph i . Molar enthalpy of fusion of the hydrogenated palm fat of $1.61 \cdot 10^5 \text{ J/mol}$ and an absolute melting temperature of 330.5 K were taken from Kloek *et al.* assuming that the solid fat crystallized in β' or recrystallized from α to β' within the 2 days of storage [53].

Samples that were subjected to the highest cooling rate (4.7 °C/min) exhibited rheological properties common for viscoelastic gel systems. Thus, the model used matched with a good accordance ($R^2 = 0.857$). At the slowest cooling rate, the phase angles confirmed that solely viscous liquids could be prepared. Thus, it is not surprising that the model only had a R^2 of 0.601. Moreover, at the mediate cooling rate of 2.6 °C/min, oil-fat dispersions transitioned from a viscous liquid to an elastic solid only at 3.5 wt%. That could be a possible explanation as to why the model did not fit very well ($R^2 = 0.498$).

Rheological results can be explained by the microstructural changes that occur in oil-fat mixtures when cooling rates are altered. Higher quantities of smaller fat crystals were formed at higher cooling rates. The increases in the overall surface area of solid lipid as a result of the decrease in lipid crystal size gives rise to more network junctions being formed [35]. Consequently, the fat crystal network is increasingly stronger causing the oil-fat mixtures to lose its suspension-like behavior and attain a plastic fat behavior [54].

The influence of cooling rates on the thermal stability of oil-fat mixtures was determined by heating the oil-fat mixtures in the rheometer (Fig. 8) and with DSC measurements (Table 2). Both, rheometer and DSC measurements confirmed that the thermal stability of the oil-fat mixtures increased with increasing palm fat concentration due to the solubility of the solid fat, regardless of the cooling rate (rheometer data not shown). Interestingly, DSC analysis showed that the thermal stability decreased with increasing cooling rates whereas opposite results were observed on the rheometer. The two higher cooling rates confirmed the results from DSC measurements and liquefaction temperature decreased with higher cooling rates. However the samples prepared at the slowest cooling rate exhibited the

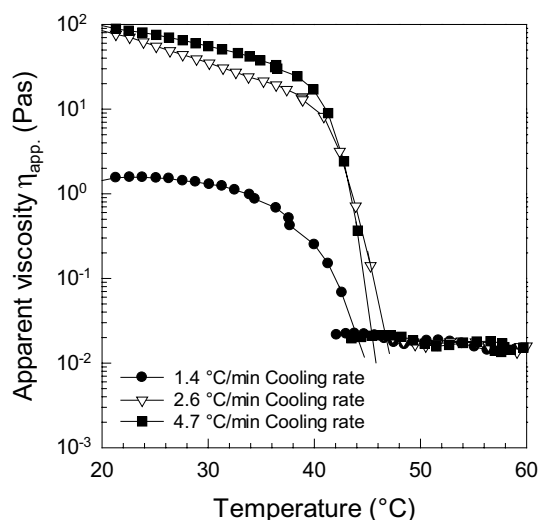


Fig. 8 Apparent viscosity η_{app} with shearing at 1 s^{-1} as function of temperature (20–60 °C) of oil-fat mixtures subjected to different cooling rates (1.4, 2.6, and 4.7 °C/min) at a palm fat concentration of 4.5 wt% in canola oil

lowest thermal stability. This may potentially be attributed to differences in heat transfer on the rheometer and the DSC since samples were sheared during heating in the rheometer but were at rest in the DSC. The oil-fat mixtures manufactured at the two higher cooling rates had markedly higher viscosities than the more slowly cooled sample up to the temperature of liquefaction, which may have influenced the heat transfer. The decrease of thermal stability with higher cooling rates may be attributed to the different crystal aggregate sizes. Larger crystal aggregates impede the heat transfer and, thus, cause higher melting points.

Moreover, the cooling rate had a substantial influence on the optical properties of the samples (Fig. 5). The normalized lightness values were highest for samples that had been cooled at the fastest cooling rate (4.7 °C/min) and lowest for samples that had been subjected to the medium cooling rate (2.6 °C/min). At a palm fat concentration of 4.5 wt%, for example, the L^*/L_0^* was 0.42, 0.38, and 0.46 for oil-fat mixtures that had been subjected to cooling rates of 1.4, 2.6, and 4.7 °C/min, respectively. These results may again be attributed to the relationship between particle size and number, as well as the intensity of light scattered [46]. Light-scattering generally increases with the increasing number of particles in the system, and increases or decreases according to a complex pattern depending on the particle size. Cooling rates may influence both the number of particles and the size of particles present in an oil-fat mixture. At higher cooling rates, smaller crystals are obtained since the degree of supercooling is greater. Therefore, more crystals must be generated at a fixed solid fat concentration. Depending on the local maxima and

minima, which depends on the scattering coefficient of the particle size, samples may thus get more or less turbid [43]. Based on our results, a cooling rate of 2.6 °C/min probably led to crystals attaining a size where scattering was close to or within a local scattering minimum.

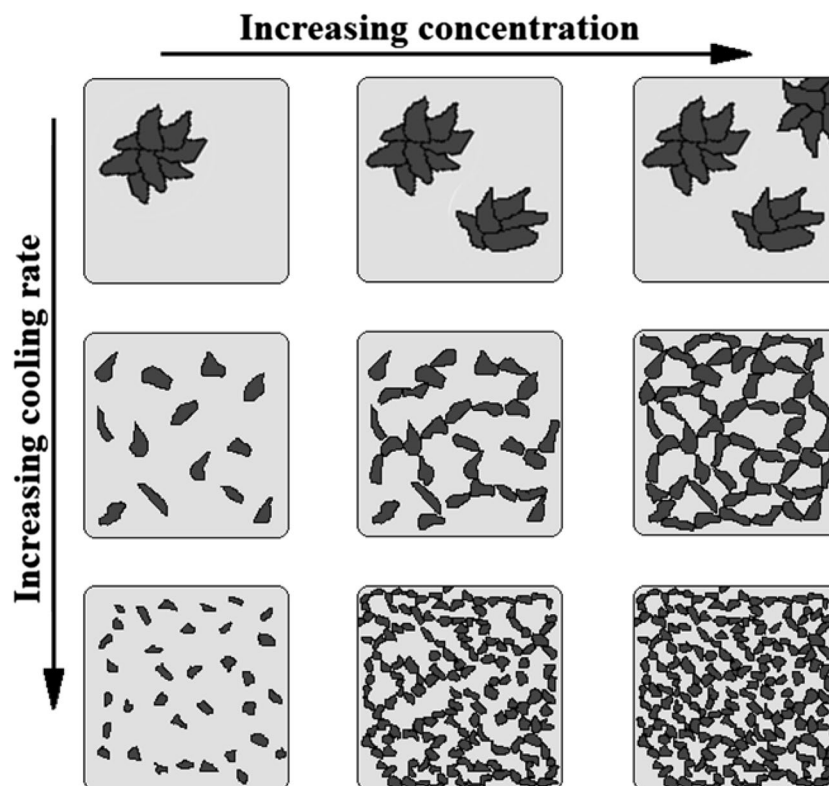
Microscopy images of oil-fat mixtures prepared at different cooling rates and with varying palm fat concentrations showed that the sizes of crystal aggregates decreased with an increasing cooling rate. Extremely large crystal spherulites with diameter sizes of approximately 50–100 μm were formed, particularly at the slow cooling rate (1.4 °C/min). By contrast, crystal aggregates had diameters of 5–10 μm or smaller at cooling rates of 2.6 and 4.7 °C/min. Image analysis demonstrated that crystal aggregates had average particle diameters that were slightly lower at 4.7 °C/min than crystals formed at 2.6 °C/min. The crystal aggregate diameters between these two cooling rates differed by 1–2 μm . A three-dimensional fat crystal network was apparent at the two higher cooling rates, whereas at the slowest cooling rate, the large crystal spherulites were not interconnected. Differences in crystal size as a function of the cooling rate have been described for lards and margarines previously, where smaller fat crystals were formed at higher cooling rates [26–28]. This may be attributed to the increased degree of supercooling which promotes the formation of a higher number of nuclei [55]. An oil-fat mixture needs to be undercooled by approx. 5 °C before fat crystal nucleation occurs [56]. The formation of stable nuclei has been attributed to changes in the Gibbs free energy due to alterations in surface and volume [53, 56, 57]. Formation of nuclei is driven by the level of supercooling [58]. The nucleation rate, i.e., the number of crystals formed per unit volume and specified time increment, can be modeled using the Gibbs-Thompson approach with the Fisher-Turnbull model [59], while crystal growth can be modeled using the Avrami equation [56, 57].

Mechanistic Model

Results of this study may be interpreted in terms of a mechanistic model shown in Fig. 9 that may be used to explain the complex behavior observed in oil-fat mixtures.

- *Slow cooling rates:* at slow cooling rates, solid fats have a tendency to precipitate from the hot liquid oil-solid fat melt in the form of large crystal spherulites consisting of individual crystal aggregates. These large spherulites move freely within the surrounding liquid oil phase, much like a suspension of solid particles or an emulsion composed of two immiscible liquid oils. With increasing concentrations of solid fat, the number of particles increases; however, since particles are larger, the num-

Fig. 9 Graphical illustration of the influences of solid fat concentration and cooling rate on the microstructure of oil-fat mixtures



ber of particles in the system is much smaller than if the particles were of smaller size. At a solid content of 2.5 wt% and an average spherulite diameter of 50 μm in 1 ml oil gel, for example, a total of 1.84×10^6 solid fat crystal spherulite would be present, while at the same concentration of fat, 1.91×10^8 of solid fat crystal aggregates of an average particle diameter of 5 μm were present (assuming that particles are spherical). An increase in fat concentration, thus, has much less effect on the microstructure of oil gels that contains large crystal aggregates, since by virtue of their smaller numbers, the fat crystal aggregates are less likely to interact and form a network. Consequently, much less effect of solid fat concentration on the physical properties of slowly cooled oil-fat mixtures may be observed.

- **High cooling rates:** at high cooling rates, solid fats have a tendency to precipitate from the hot liquid oil-solid fat melt in the form of small crystal aggregates. These smaller crystals aggregates are present in the oil-fat mixtures in greater numbers than in oil-fat mixtures that have been cooled less rapidly and that contain the same solid fat concentration (see above). The small crystal aggregates are more likely to interact and form networks, even at low solid fat concentrations. By virtue of their high numbers, oil-fat mixtures fabricated with high cooling rates thus display a high sensitivity to solid fat concentration, i.e., their physicochemical properties

may change significantly when the solid fat concentration is altered.

Conclusions

Our results show that rheology, appearance, and thermal stability of oil-fat mixtures depend on both palm fat concentration and cooling rate. Because of this, it proves to be difficult or even impossible to have the systems simultaneously display a desired mechanical, optical or thermal behavior. For example, oil-fat gels may be manufactured that have specific viscoelastic properties. Thus, oil-fat gels may be prepared that might be able to keep particulates, such as salt and spices, in suspension, one of the main requirements for oil-based marinades. Their appearance, however, which is another key functional property, can range from being completely transparent (desirable) to being very opaque and having an almost whitish color (undesired). Furthermore, the systems are to remain stable over a broad temperature range if they are used as marinades, particularly in the summer grilling season. Unfortunately, their thermal stability of the here investigated system may only be altered by a few degrees by altering the cooling rate with which oil-fat mixtures are manufactured. It is therefore unavoidable that manufacturers find local optima in the different

physical properties in which they are interested. These correspond to a particular microstructure that may then be generated by a specific process (e.g., a specific cooling rate). If manufacturers require higher thermal stabilities, fats with higher melting points will need to be used. It should be noted though that the microstructure of these oil-fat mixtures is likely going to be quite different from the ones reported in this study, and as such the oil-fat mixtures will have different physicochemical properties. Taken together, this study therefore highlights the complexity and difficulty encountered when designing multifunctional oil-fat gels, a fact that should be of high relevance to food manufacturers.

Acknowledgments We would like to thank Scheid AG for their financial support of this study and the fruitful discussion of oil-fat mixtures as the basis of marinades. We would also like to thank Cognis for their donation of the palm fat used in this study. Finally, we appreciate assistance of Thrandur Helgason and Valerie Schuh in conducting the thermal and optical studies.

References

1. Yusop SM, O'Sullivan MG, Kerry JP (2011) Marinating and Enhancement of the Nutritional Content of Processed Meat Products. In: Kerry JP, Kerry JF (eds) *Processed Meats: Improving Safety, Nutrition and Quality*. Woodhead Publishing, Cambridge, pp 421–449
2. Feiner G (2006) *Meat Products Handbook: Practical Science and Technology*. Woodhead Publishing, Cambridge
3. McEvoy JH (2003) The Might of Marinades. *Prepared Foods* 172:49–58
4. Xiong YL, Mikel WB (2001) Meat and Meat Products. In: Hui YH, Nip W-K, Rogers RW, Young OA (eds) *Meat Science and Applications*. Marcel Dekker, New York, pp 351–370
5. Perneti M, van Malssen KF, Flöter E, Bot A (2007) Structuring of Edible Oils by Alternatives to Crystalline Fat. *Curr Opin Colloid Interface Sci* 12:221–231
6. Vintiloiu A, Leroux J-C (2008) Organogels and Their Use in Drug Delivery—a Review. *J Controlled Release* 125:179–192
7. Bot A, Veldhuizen YSJ, den Adel R, Roijers EC (2009) Non-Tag Structuring of Edible Oils and Emulsions. *Food Hydrocolloids* 23:1184–1189
8. Rogers MA (2009) Novel Structuring Strategies for Unsaturated Fats—Meeting the Zero-Trans, Zero-Saturated Fat Challenge: A Review. *Food Res Int* 42:747–753
9. Co ED, Marangoni AG (2012) Organogels: An Alternative Edible Oil-Structuring Method. *J Am Oil Chem Soc* 89:749–780
10. Narine SS, Marangoni AG (1999) Relating Structure of Fat Crystal Networks to Mechanical Properties: A Review. *Food Res Int* 32:227–248
11. Kloek W, Walstra P, Vliet T (2000) Nucleation Kinetics of Emulsified Triglyceride Mixtures. *J Am Oil Chem Soc* 77:643–652
12. Kloek W, van Vliet T, Walstra P (2005) Mechanical Properties of Fat Dispersions Prepared in a Mechanical Crystallizer. *J Texture Stud* 36:544–568
13. Walstra P (2003) *Physical Chemistry of Foods*. Marcel Dekker, New York
14. Vreeker R, Hoekstra LL, den Boer DC, Agterof WGM (1992) The Fractal Nature of Fat Crystal Networks. *Colloids and Surf* 65:185–189
15. Van den Tempel M (1961) Mechanical Properties of Plastic-Disperse Systems at Very Small Deformations. *J Colloid Sci* 16:284–296
16. Tang D, Marangoni AG (2006) Quantitative Study on the Microstructure of Colloidal Fat Crystal Networks and Fractal Dimensions. *Adv Colloid Interface Sci* 128–130:257–265
17. Marangoni AG, Tang D (2008) Modeling the Rheological Properties of Fats: A Perspective and Recent Advances. *Food Biophys* 3:113–119
18. Kloek W, van Vliet T, Walstra P (2005) Large Deformation Behavior of Fat Crystal Networks. *J Texture Stud* 36:516–543
19. Acevedo NC, Marangoni AG (2010) Characterization of the Nanoscale in Triacylglycerol Crystal Networks. *Cryst Growth Des* 10:3327–3333
20. Acevedo NC, Marangoni AG (2010) Toward Nanoscale Engineering of Triacylglycerol Crystal Networks. *Cryst Growth Des* 10:3334–3339
21. Acevedo NC, Peyronel F, Marangoni AG (2011) Nanoscale Structure Intercrystalline Interactions in Fat Crystal Networks. *Curr Opin Colloid Interface Sci* 16:374–383
22. Kamphuis H, Jongschaap RJJ (1985) The Rheological Behaviour of Suspensions of Fat Particles in Oil Interpreted in Terms of a Transient-Network Model. *Colloid Polym Sci* 263:1008–1024
23. Papenhuijzen JMP (1972) The Role of Particle Interactions in the Rheology of Dispersed Systems. *Rheol Acta* 11:73–88
24. Sherman P (1968) The influence of particle size on the viscoelastic properties of flocculated emulsions. 5th International Conference on Rheology, Kyoto, Japan, pp. 327–338
25. Marangoni AG, Rousseau D (1996) Is Plastic Fat Rheology Governed by the Fractal Nature of the Fat Crystal Network? *J Am Oil Chem Soc* 73:991–994
26. Campos R, Narine SS, Marangoni AG (2002) Effect of Cooling Rate on the Structure and Mechanical Properties of Milk Fat and Lard. *Food Res Int* 35:971–981
27. Pérez-Martínez D, Alvarez-Salas C, Charó-Alonso M, Dibildox-Alvarado E, Toro-Vazquez JF (2007) The Cooling Rate Effect on the Microstructure and Rheological Properties of Blends of Cocoa Butter with Vegetable Oils. *Food Res Int* 40:47–62
28. Pérez-Martínez D, Alvarez-Salas C, Morales-Rueda JA, Toro-Vazquez JF, Charó-Alonso M, Dibildox-Alvarado E (2005) The Effect of Supercooling on Crystallization of Cocoa Butter-Vegetable Oil Blends. *J Am Oil Chem Soc* 82:471–479
29. DeMan JM (1964) Effect of Cooling Procedures on Consistency, Crystal Structure and Solid Fat Content of Milk Fat. *Dairy Ind* 29:244–246
30. Awad TS, Rogers MA, Marangoni AG (2004) Scaling Behavior of the Elastic Modulus in Colloidal Networks of Fat Crystals. *J Phys Chem B* 108:171–179
31. Higaki K, Sasakura Y, Koyano T, Hachiya I, Sato K (2003) Physical Analyses of Gel-Like Behavior of Binary Mixtures of High- and Low-Melting Fats. *J Am Oil Chem Soc* 80:263–270
32. Higaki K, Koyano T, Hachiya I, Sato K (2004) In Situ Optical Observation of Microstructure of β -Fat Gel Made of Binary Mixtures of High-Melting and Low-Melting Fats. *Food Res Int* 37:2–10
33. Higaki K, Koyano T, Hachiya I, Sato K, Suzuki K (2004) Rheological Properties of β -Fat Gel Made of Binary Mixtures of High-Melting and Low-Melting Fats. *Food Res Int* 37:799–804
34. Cornily G, Meste ML (1985) Flow Behaviour of Lard and of Its Fractions at 15°C. Relationship with Thermal Behaviour and Chemical Composition. *J Texture Stud* 16:383–402
35. Davis SS (1973) Rheological Properties of Semi-Solid Foodstuffs—Viscoelasticity and Its Role in Quality Control. *J Texture Stud* 4:15–40
36. Pollitt RJM (1974) Oils and Fats Group Symposium: Rheology of Shortenings. *J Sci Food Agric* 25:885–887

37. de Man JM, Beers AM (1987) Fat Crystal Networks: Structure and Rheological Properties. *J Texture Stud* 18:303–318
38. Nederveen CJ (1963) Dynamic Mechanical Behavior of Suspensions of Fat Particles in Oil. *J Colloid Sci* 18:276–291
39. Heertje I (1993) Microstructural Studies in Fat Research. *Food Struct* 12:77–94
40. Tadros TF (2010) *Rheology of Dispersions*. Wiley-VCH, Weinheim
41. Mezger TG (2006) *The rheology handbook*. Vincentz Network, Hannover
42. Marangoni AG, Acevedo N, Maleky F, Co ED, Peyronel F, Mazzanti G, Quinn B, Pink D (2012) Structure and Functionality of Edible Fats. *Soft Matter* 8:1275–1300
43. Weiss J, Liao W (2000) Addition of Sugars Influences Color and Appearance of Oil-in-Water Emulsions. *J Agric Food Chem* 48:5053–5058
44. Omar Z, Chong CL, Cheow CS, Rashid NA (2005) Crystallisation and Rheological Properties of Hydrogenated Palm Oil and Palm Oil Blends in Relation to Crystal Networking. *Eur J Lipid Sci Technol* 107:634–640
45. Knoester M, de Bruijne P, van Den Tempel M (1972) The Solid-Liquid Equilibrium of Binary Mixtures of Triglycerides with Palmitic and Stearic Chains. *Chem Phys Lipids* 9:309–319
46. McClements DJ, Chantrapornchai W, Clydesdale F (1998) Prediction of Food Emulsion Color Using Light Scattering Theory. *J Food Sci* 63:935–939
47. Chantrapornchai W, Clydesdale F, McClements DJ (1998) Influence of Droplet Size and Concentration on the Color of Oil-in-Water Emulsions. *J Agric Food Chem* 46:2914–2920
48. Graessley WW (1967) Viscosity of Entangling Polydisperse Polymers. *J Chem Phys* 47:1942–1953
49. Lu Y, An L, Wang S-Q, Wang Z-G (2014) Origin of Stress Overshoot During Startup Shear of Entangled Polymer Melts. *ACS Macro Lett* 3:569–573
50. Weiss J, McClements DJ (2000) Influence of Ostwald Ripening on Rheology of Oil-in-Water Emulsions Containing Electrostatically Stabilized Droplets. *Langmuir* 16:2145–2150
51. Shih W-H, Shih WY, Kim S-I, Liu J, Aksay IA (1990) Scaling Behavior of the Elastic Properties of Colloidal Gels. *Phys Rev A* 42:4772–4779
52. Bremer LGB, van Vliet T, Walstra P (1989) Theoretical and Experimental Study of the Fractal Nature of the Structure of Casein Gels. *J Chem Soc, Faraday Trans 1*(85):3359–3372
53. Kloek W, Walstra P, Vliet T (2000) Crystallization Kinetics of Fully Hydrogenated Palm Oil in Sunflower Oil Mixtures. *J Am Oil Chem Soc* 77:389–398
54. Metzroth DJ (2005) Shortenings: Science and Technology. In: Shahidi F (ed) *Bailey's Industrial Oil and Fat Products*. John Wiley, Hoboken, pp 83–123
55. Weiss J, Decker EA, McClements J, Kristbergsson K, Helgason T, Awad TS (2008) Solid Lipid Nanoparticles as Delivery Systems for Bioactive Food Components. *Food Biophys* 3:146–154
56. Rogers MA, Tang D, Ahmadi L, Marangoni AG (2007) Fat Crystal Networks. In: Aguilera JM, Lillford PJ (eds) *Food Materials Science: Principles and Practice*. Springer Science and Business Media, New York, pp 370–414
57. Marangoni AG (2005) Crystallization Kinetics. In: Marangoni AG (ed) *Fat Crystal Networks*. Marcel Dekker, New York, pp 21–82
58. Hartel R (2007) The Crystalline State. In: Aguilera JM, Lillford PJ (eds) *Food Materials Science: Principles and Practice*. Springer Science & Business Media, New York, pp 45–66
59. Marangoni AG, Ollivon M (2007) Fractal Character of Triglyceride Spherulites Is a Consequence of Nucleation Kinetics. *Chem Phys Lett* 442:360–364